Adv. Space Res. Vol.4, No.7, pp.179-182, 1984
Printed in Great Britain.

0273-1177/84 $0.00 + .50

POST-FLARE THERMAL WAVES IN THE SOLAR CORONA

Zdenek Švestka

Laboratory for Space Research, Utrecht, Beneluxlaan 21, 3527 HS Utrecht, The Netherlands

ABSTRACT

While imaging giant post-flare arches in the solar corona, the Hard X-Ray Spectrometer aboard the SMM detected thermal disturbances propagating through the corona after two-ribbon flares. The speed of propagation is close to, or below, 10 km s^{-1}, and no obvious time-variation of the speed is indicated in the HXIS data. For subsequent two-ribbon flares in the same active region, these thermal disturbances (waves) exhibit highly homologous properties; thus the waves appear to propagate through preexisting arches formed after earlier flares. Temperatures of > 20 x 10^6 K have been detected in these moving phenomena. We suggest that we see here in X-rays upper products of the consecutive reconnections which create the post-flare loops below. Temperature maps in fine field of view of HXIS offer now a new possibility to detect postflare arches in the corona built during two-ribbon flares.

1. POST-FLARE ARCHES OF 6 AND 7 NOVEMBER 1980

Figure 1 shows the sequence of coronal arches imaged by the Hard X-ray Imaging Spectrometer (HXIS) in > 3.5 keV X-rays on 6 and 7 November 1980, and Figure 2 presents X-ray images of the arches Nos. 1 and 2. All three arches were initiated by two-ribbon flares in the underlying active region and the striking homology of the arches 1 and 2 in Figure 2 suggests that the arch No. 2 was a revival of the Arch No. 1 /1/. Since another major two-ribbon flare occurred in the same active region at 13:41 UT on November 5, it is likely that also the first arch in Figure 1 was the revival of a preexisting coronal feature. (HXIS began to look at the active region only at 06:24 UT on November 6.).

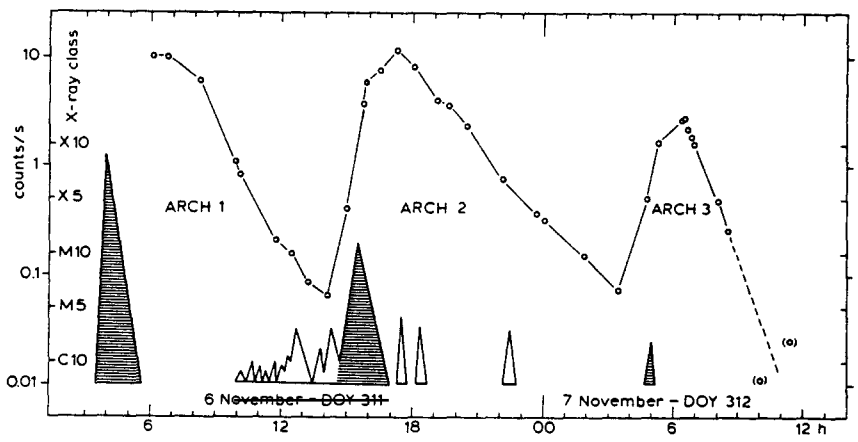

Fig. 1. Time variations of the brightness of the coronal arch on 6 and 7 November 1980: maximum counts per second in one pixel of HXIS coarse field of view (32"x32") within the arch. Energy range 3.5 - 5.5 keV. The triangles below indicate 1 - 8 Å X-ray variations in the underlying active region (GOES-2 data): scale C6 - X10. The hatched triangles are the flares that enhanced the arches.

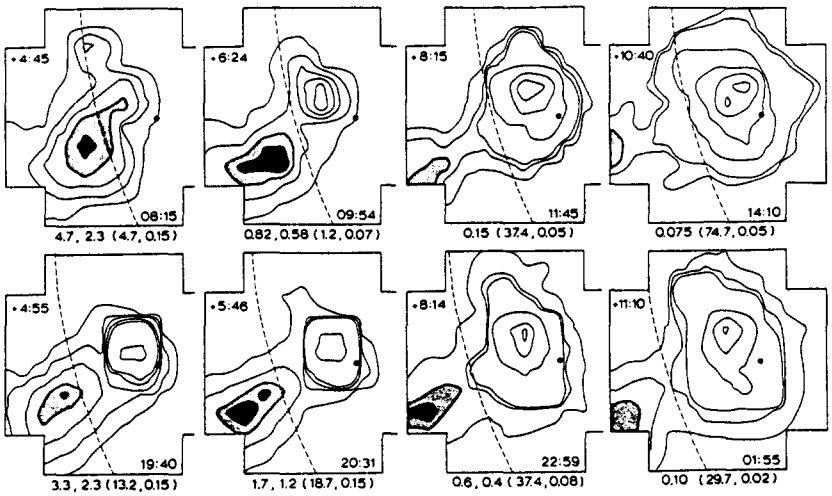

Fig. 2. 3.5 - 5.5 keV X-ray images of the arches 1 and 2 of Figure 1. The dashed line is the solar limb, a black dot marks the largest spot in the underlying active region. In each image the lower-right number is the time of imaging, while the upper-left number is the time elapsed from the onset of the parent flare. Coarse field of view: 32" resolution. The numbers below each image are counts s^{-1} per pixel corresponding to the brightest (shaded) contour(s) in the arch and, in brackets, the maximum en minimum contours in the image.

2. IMAGES IN COARSE FIELD OF VIEW

On 22 May 1980 HXIS observed another post-flare arch of a similar kind which was a stationary formation, with its brightness maximum staying at a constant projected distance of 100000 km from the $H_{||} = 0$ line, corresponding to an altitude of ~ 150000 km /2/. In contrast to that, as Figure 2 demonstrates, in the arches of November 6 and 7, 1980, brightness maxima moved upwards. A detailed analysis of HXIS images in the coarse field of view reveals that there were two velocity components in the arches (Figure 3): a slow one, with 8 - 12 km s^{-1} in projection on the plane of the sky, and a fast one, with ~ 35 km s^{-1}. The slower speed is related to the rise of the brightness maxima whereas the source of the fast component remains unknown.

The best data is available for the arch No. 2. At the projected altitude of 100000 km (± 25000 km, mean of six integrated HXIS pixels) temperature (~ 14 x 10^6 K) peaked about 1 hour, X-ray counts about 2 hours, and emission measure about 3.5 hours after the onset of the arch revival (as determined from the count ratio in the energy bands of 5.5-8.0 keV and

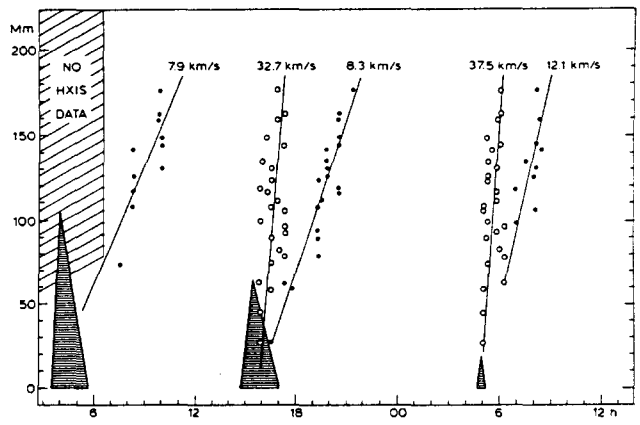

Fig. 3. Velocities deduced from a set of 25 pixels of HXIS coarse field of view. Each point (or circle) shows the time at which the arch brightness reached maximum in a HXIS pixel located at a given projected distance (in Mm) from the active region. The triangles (parent flares) have been taken from Figure 1.

3.5-5.5 keV). The temperature began to rise at the very onset of the flare that revived the arch. This is an evidence that since its beginning the revived arch was fed with energy within the whole extent of the preexisting arch; thus the revival probably means a refill of the preexisting arch with heated plasma.

In addition to that, however, the images in Figure 2 and the velocity patterns in Figure 3 reveal that a new feature was formed in the low corona and propagated upwards. According to Figure 3, the slowly moving feature (with speed of 8.3 km s^{-1}) passed through the integrated six pixels in the arch between 18:20 and 20:00 UT. During the same period the decrease in temperature stopped and the temperature stayed at a value close to 10 x 10^6 K before it began to decrease again between 19:50 and 20:30 UT /1/. The emission measure peaked at about 18:10 UT and continuously decreased after that. This behaviour of temperature and emission measure leads to the assumption that the travelling disturbance was predominantly a temperature enhancement.

3. TEMPERATURE MAPS

In the coarse field of view of HXIS, the maximum temperature in the arch is always observed slightly above the site of its maximum brightness and shifts upwards with a similar speed. This can be interpreted as a sequential heating of the arch at progressively higher altitudes by the propagating disturbance, while density in the arch decreases with the height /1/. The arch must cool very slowly by radiation (with $n_e \sim 10^9$ cm^{-3} and conductive cooling inhibited), since otherwise its energy content would exceed that of the flare below.

The rising wave can be recognized and studied even in the early phase of the arch development in HXIS fine field of view. Whereas the image of the arch cannot be easily discriminated and detached from the image of the underlying flare, temperature maps show clearly an enhanced temperature in the arch above the flare site and a propagation of the enhanced region upwards (Figure 4). We have integrated the areas within the 14 x 10^6 K isotherm, and deduced from them the speed of the thermal wave during this period: it results as 7.4 km s^{-1}, in reasonable agreement with the average speed of 8.3 km s^{-1} found from Figure 3.

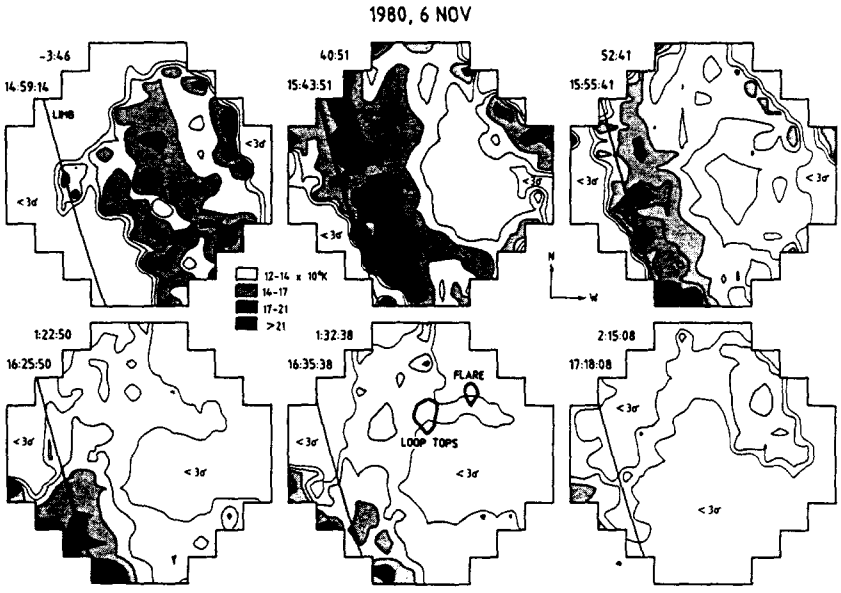

Fig. 4. Temperature maps of the early phase of the arch No. 2 of Figure 1, in HXIS fine field of view (8" resolution). The contours correspond to 10, 12, 14, 17, and 21 x 10^6 K, as determined from the ratio of counts in the 5.5-8.0 keV and 3.5-5.5 keV energy bands. Only ratios with > 3σ statistical significance have been used for these plots. Therefore, the temperature is unknown whereever the ratio was < 3σ and the computer-made isotherms at the boundaries of these regions are fictitious. The original flare site and the top of X-ray loops later on are indicated in one frame. Time data give the UT (below) and time difference from the maximum of the impulsive phase of the flare (above).

Small areas in the arch show temperatures in excess of 21 x 10^6 K, much higher than the temperature values deduced from the coarse field of view. Since one pixel of coarse FOV integrates 16 pixels of fine FOV of HXIS, these small hot regions merge with their surroundings in the coarse FOV, so that the coarse maps obviously underestimate the peak temperature.

Shortly after the last picture of Figure 4, at 17:24 UT, another important flare appeared in the same active region. It was classified as 2B in H alpha, but it was a compact flare, without any growing system of loops in the corona. This flare did not produce any thermal enhancement of the kind demonstrated in Figure 4. On the other hand, we got very similar maps for another two-ribbon flare on 4 June 1980. The speed of the thermal wave there was ~ 6.3 km s^{-1}. HXIS looked at this flare for one orbit only; still, the existence of a thermal wave moving upwards with a speed similar to that on November 6, indicates strongly that this flare, too, was the source of a post-flare arch. This offers an attractive possibility to detect more arches from HXIS data even when the arch itself, in the post-flare phase, was not imaged as HXIS looked elsewhere on the Sun.

4. INTERPRETATION

The observations show clearly that the post-flare X-ray arches must be natural components of two-ribbon flares, formed or revived during the flare formation: at the same time as flare loops are formed below (sometimes for hours after the flare onset), the arch originates in the corona above them, through reconnection of distended field lines, as suggested by Kopp and Pneuman /3/, Anzer and Pneuman /4/, and Svestka et al. /2/. If an old arch still does exist when a new two-ribbon flare occurs below it, like in Figure 1, the loop distention at the onset of the flare is hindered by the arch structure and at least some extending field lines reconnect with field lines in the arch. Thus particles accelerated in the reconnection process as well as heated plasma from below begin to have free access into the preexisting arch and its temperature begins to rise: the arch revival begins. However, this slowing down of the "field opening" delays the subsequent Kopp-Pneuman reconnection and the formation of new flare loops /1/. Only after the time of the first post-flare loop appearance a new arch begins to be formed as the upper product of the loop-reconnection process, and the velocities found in Figure 3 might reflect this formation.

One may be tempted to interpret the temperature maps in Figure 4 as products of sequential arch cooling, starting from below and proceeding upwards. Also the constant speed of the rise of maximum brightness in Figure 3 could be explained if n_e is inversely proportional to the altitude, h, and the arch cools through radiation. However, the densities then needed for the interpretation of Figure 4, $n_e \simeq 5 \times 10^{10}$ cm^{-3} at $h \simeq 40000$ km, seem too high; and, in particular, the fact that HXIS recorded a break in the cooling process when the travelling disturbance passed through the analysed range of altitudes (cf. Section 3) contradicts this supposition. Thus we are left with a thermal wave travelling with a constant speed of ~ 8 km s^{-1} through an arch in which the density decreases upwards. Maximum temperature and density at $h \simeq 100000$ km in this arch has been estimated to $\gtrsim 14 \times 10^6$ K and $\sim 2.4 \times 10^9$ cm^{-3} /1/. This corresponds to a sound speed well above 400 km s^{-1} and an Alfvén speed of 44 km s^{-1} for a magnetic field strength of 1 gauss. Therefore, it looks likely that the much lower speed we find is related in some way to the reconnection process itself.

ACKNOWLEDGEMENT

The development and construction of HXIS /5/ was made possible by support from the Netherlands Ministry for Education and Science, and the Science and Engineering Research Council of the United Kingdom.

REFERENCES

1. Z. Svestka, Revivals of a Coronal Arch, submitted to Solar Phys. (1984)

2. Z. Svestka, R.T. Stewart, P. Hoyng, W. van Tend, L.W. Acton, A.H. Gabriel, C.G. Rapley, A. Boelee, E.C. Brunner, C. de Jager, H. Lafleur, G. Nelson, G.M. Simnett, H.F. Van Beek, and W.J. Wagner, Observations of a Post-Flare Radio Burst in X-Rays, Solar Phys. 75, 305 (1984)

3. R.A. Kopp and G.W. Pneuman, Magnetic Reconnection in the Corona and the Loop Prominence Phenomenon, Solar Phys. 50, 85 (1976)

4. U. Anzer and G.W. Pneuman, Magnetic Reconnection and Coronal Transients, Solar Phys. 79, 129 (1982)

5. H.F. van Beek, P. Hoyng, H. Lafleur, and G.M. Simnett, The Hard X-Ray Imaging Spectrometer (HXIS), Solar Phys. 65, 39 (1980)